AFRL-RY-WP-TR-2021-0269

RECONFIGURABLE ANTENNA ARRAY USING THE PIN-DIODE-SWITCHED PRINTED SQUARE SPIRAL ELEMENT

Corey M. Stamper
Wright State University

OCTOBER 2021
Final Report

DISTRIBUTION STATEMENT A. Approved for public release; distribution is unlimited.
See additional restrictions described on inside pages

STINFO COPY

AIR FORCE RESEARCH LABORATORY
SENSORS DIRECTORATE
WRIGHT-PATTERSON AIR FORCE BASE, OH 45433-7320
AIR FORCE MATERIEL COMMAND
UNITED STATES AIR FORCE

REPORT DOCUMENTATION PAGE

Form Approved
OMB No. 0704-0188

1. REPORT DATE *(DD-MM-YY)*	2. REPORT TYPE	3. DATES COVERED *(From - To)*
October 2021	Thesis	5 October 2021 –5 October 2021

4. TITLE AND SUBTITLE
RECONFIGURABLE ANTENNA ARRAY USING THE PIN-DIODE-SWITCHED PRINTED SQUARE SPIRAL ELEMENT

5a. CONTRACT NUMBER N/A
5b. GRANT NUMBER
5c. PROGRAM ELEMENT NUMBER N/A

6. AUTHOR(S)
Corey M. Stamper

5d. PROJECT NUMBER N/A
5e. TASK NUMBER N/A
5f. WORK UNIT NUMBER N/A

7. PERFORMING ORGANIZATION NAME(S) AND ADDRESS(ES)
Wright State University
3640 Colonel Glenn Hwy.
Dayton, OH 45435

8. PERFORMING ORGANIZATION REPORT NUMBER

9. SPONSORING/MONITORING AGENCY NAME(S) AND ADDRESS(ES)
Air Force Research Laboratory, Sensors Directorate
Plans Branch (AFRL/RYZC)
Sensors Plans & Advanced Programs Division
Wright-Patterson Air Force Base, OH 45433-7320
Air Force Materiel Command, United States Air Force

10. SPONSORING/MONITORING AGENCY ACRONYM(S)
AFRL/RYDI

11. SPONSORING/MONITORING AGENCY REPORT NUMBER(S)
AFRL-RY-WP-TP-2021-0269

12. DISTRIBUTION/AVAILABILITY STATEMENT
DISTRIBUTION STATEMENT A. Approved for public release; distribution is unlimited.

13. SUPPLEMENTARY NOTES
PAO case number AFRL-2021-3270, Clearance Date 5 October 2021. A thesis submitted in partial fulfillment of the requirements for the degree of Master of Science in Engineering at Wright State University. This work was funded in whole or in part by Department of the Air Force contract. The U.S. Government has for itself and others acting on its behalf an unlimited, paid-up, nonexclusive, irrevocable worldwide license to use, modify, reproduce, release, perform, display, or disclose the work by or on behalf of the U. S. Government. Report contains color.

14. ABSTRACT
A dual-band array of reconfigurable elements is modeled and simulated. The array consists of four single square spiral microstrip antennas that are corporately fed and are used as a unit cell. The single square spiral uses two PIN diodes as switching elements to achieve reconfiguration. The array has four switch states that can operate over four discrete frequencies in the S and C bands. The unit cell radiation pattern is used with the pattern multiplication model to quickly simulate the array pattern of larger arrays. A 3 x 3 array of the unit cells is modeled with only the center element active and designated as the embedded unit cell. The embedded unit cell is used to capture the effects of mutual coupling and to see how significantly the coupling affects the radiation patterns. The effects of mutual coupling are found to be negligible for a 2 x 2 and larger sized arrays.

15. SUBJECT TERMS
antenna array, machine learning, PIN-diode-switched printed square spiral element , reconfigurable

16. SECURITY CLASSIFICATION OF:			17. LIMITATION OF ABSTRACT:	18. NUMBER OF PAGES	19a. NAME OF RESPONSIBLE PERSON (Monitor)
a. REPORT	b. ABSTRACT	c. THIS PAGE			William Gouty
Unclassified	Unclassified	Unclassified	SAR	52	19b. TELEPHONE NUMBER *(Include Area Code)* N/A

Reconfigurable Antenna Array Using the PIN-Diode-Switched Printed Square Spiral Element

A thesis submitted in partial fulfillment
of the requirements for the degree of
Master of Science in Engineering

by

COREY M. STAMPER
B.S.E.E., Wright State University, 2020

2021
Wright State University

Wright State University
GRADUATE SCHOOL

September 17, 2021

I HEREBY RECOMMEND THAT THE THESIS PREPARED UNDER MY SUPERVISION BY Corey M. Stamper ENTITLED Reconfigurable Antenna Array Using the PIN-Diode-Switched Printed Square Spiral Element BE ACCEPTED IN PARTIAL FULFILLMENT OF THE REQUIREMENTS FOR THE DEGREE OF Master of Science in Engineering.

Michael A. Saville, Ph.D., P.E.
Thesis Director

Brian D. Rigling, Ph.D.
Interim Chair, Department of Electrical Engineering

Barry Milligan, Ph.D.
Dean of the Graduate School

Committee on
Final Examination

Michael A. Saville, Ph.D., P.E.

Joshua Ash, Ph.D.

Yan Zhuang, Ph.D.

ABSTRACT

Stamper, Corey. M.S.Egr., Department of Electrical Engineering, Wright State University, 2021.
Reconfigurable Antenna Array Using the PIN-Diode-Switched Printed Square Spiral Element.

A dual-band array of reconfigurable elements is modeled and simulated. The array consists of four single square spiral microstrip antennas that are corporately fed and are used as a unit cell. The single square spiral uses two PIN diodes as switching elements to achieve reconfiguration. The array has four switch states that can operate over four discrete frequencies in the S and C bands. The unit cell radiation pattern is used with the pattern multiplication model to quickly simulate the array pattern of larger arrays. A 3 x 3 array of the unit cells is modeled with only the center element active and designated as the embedded unit cell. The embedded unit cell is used to capture the effects of mutual coupling and to see how significantly the coupling affects the radiation patterns. The effects of mutual coupling are found to be negligible for a 2 x 2 and larger sized arrays.

Contents

List of Figures

List of Tables

Acknowledgment

I would like to thank my thesis advisor Dr. Michael A. Saville, I appreciate all your help and guidance through this whole process. I have learned a lot from working with you. It has been a privilege and an honor. I would like to thank Dr. Yan Zhuang and Dr. Josh Ash for taking the time to be on my committee. I would like to thank Garrett Harris for being supportive and always willing to help out. I would like to extend my gratitude to the Electrical Engineering department at Wright State University for making my experience here a positive one. I have met many knowledgeable and inspiring people here.

Dedicated to

My family

Introduction

1.1 Motivation

It was reported by the Federal Communications Commission (FCC) that 70% of the spectrum consists of idle gaps known as white spaces that are being unused [3]. A proposed solution to improve the spectrum usage would be to use a communication protocol allowing for spectrum sharing [4]. The technology that would enable the use of this protocol is called a cognitive radio. The cognitive radio concept can be established with a software defined radio and machine learning algorithms such as convolution neural networks (CNN). The cognitive radio would facilitate the usage of the spectrum sharing process. The cognitive radio would consist of a sensing antenna and a reconfigurable antenna. The sensing antenna is used to continuously scan for unused frequency channels. The reconfigurable antenna is used to transmit and receive in the required channels. The reconfigurable antenna is used in the communication process by changing the radiation characteristics of the antenna. Reconfigurable antennas are attractive because they enhance the functionality of regular antennas by allowing the characteristics of the antenna to change on demand. Reconfigurable antennas can be used to change the frequency of operation, radiation pattern and or polarization of an antenna. Reconfiguration is achieved by connecting or disconnecting antenna segments and by redistributing antenna currents. An antenna that can be reconfigured is beneficial because it allows for a single antenna to perform multiple functions by dynamically changing the properties of the antenna. By making use of a single antenna that can perform multiple functions the overall size, space and cost of a system can be reduced. A reconfigurable antenna must be able to dynamically change its properties. In order to do this the current distribution over the volume of the antenna needs to be changed. The geometry of the antenna can be changed by switching on and off different segments of the antenna. There are a variety of techniques that can be used to reconfigure an antenna. Switching elements can be used such as PIN diodes, varactor diodes and RF-MEMS devices to change the current distribution across the radiating elements. These switches can be placed at specific locations on the antenna to reconfigure the antenna to operate at a desired frequency.

Reconfigurable antennas have been studied for several years [4]. Reconfigurable antennas have the capability to perform multiple functions by dynamically changing the properties of the antenna. These properties include operating frequency, polarization, and radiation pattern. This technology can be used to advance phased-array, communications and radar systems. In any wireless channel the effects of multipath interference are present. This multipath interference occurs with the constructive and destructive addition of signals in the path. The use of multiple-input multiple-output (MIMO) based techniques can help with the problem of multipath. MIMO allows data to be transmitted and received over multiple antennas. The use of multiple antennas will improve the chance of receiving a good representation of the data.

The focus of this effort is on the analysis of a reconfigurable antenna array that can be used as a part of the enabling technology for a cognitive radio. In this work we model and simulate a two-by-two reconfigurable microstrip square spiral antenna array that will serve as a base element for a larger array. The single element of the base antenna is a design presented in [2]. The single square microstrip antenna can be seen in Figure 1.1. The figure shows the layout of the antenna with dimensions. The analysis of the antenna performance is presented for several array sizes and switch states.

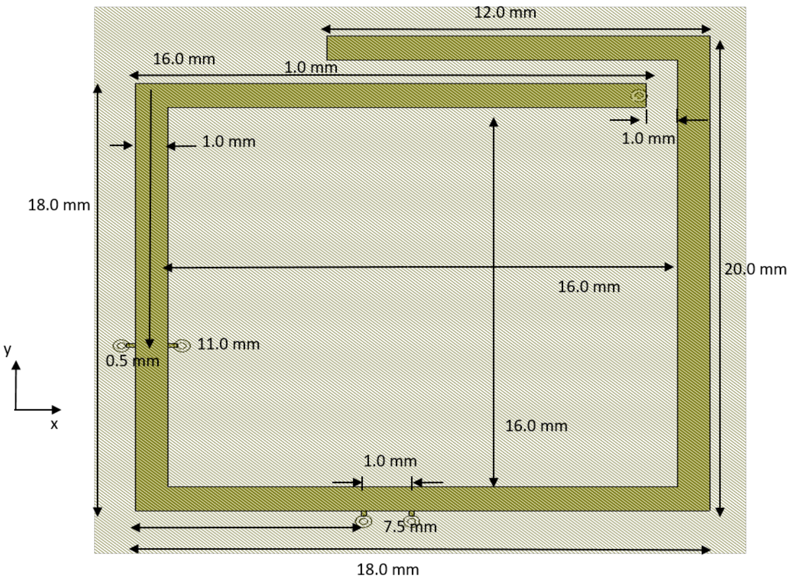

Figure 1.1: Single Square Spiral.

1.2 Challenges

Designing large arrays of element-wise transceivers is not without challenges. Some challenges in the design process include the use of biasing lines for the PIN diodes. The layout and design of the biasing lines need to be taken into consideration. These biasing lines add weight to the array and take up additional space in the array. The biasing lines can cause mutual coupling with the radiating elements that can distort and degrade the array patterns. The biasing lines need to be designed so that they do not add interference with the radiating elements. The layout of large arrays needs to be considered for spacing constraints. The spacing of each individual element in the array also needs to be considered. The mutual coupling between elements of the array should not cause too much interference with each other. The feeding of each element of the base array is going to require consideration. The feed network needs to feed all the elements from a single source. The design of the feed network needs to be impedance matched to the antenna to avoid poor radiation.

1.3 Research Hypothesis

In this work we present the analysis of a reconfigurable antenna array that is based of the work done by Huff [2]. We will model and simulate a 2 x 2 unit cell that consists of single square spiral microstrip antennas. Using a CAD program we can study the antenna and see how it performs under differernt switch conditions. We will use a pattern multiplication model to generate the patterns of larger arrays using a base array as a unit cell. The radiation patterns generated using the pattern multiplication model will be compared to the synthetic array patterns generated from CAD modeling and simulation software. The pattern multiplication will be done using an isolated element pattern and an embedded element pattern. Using this approach we can attempt to see the affects that mutual coupling has on the performance of the array. We would like to address the question of how much does mutual coupling degrade the performance of the pattern multiplication model.

1.4 Outline of Thesis

The organization of the thesis is as follows. In Chapter 2 a survey of literature was done to gain an understanding of the current state of the art of reconfigurable antennas. These previous works highlight some of the uses of reconfigurable antennas and the methods used to achieve reconfiguration. In Chapter 3 the approach that we used for modeling and simulation are described. The analysis methods that we used are explained. Chapter 4 presents the results that were obtained in the modeling and simulation process. The data from the synthetic array patterns and the pattern multiplication model are compared for arrays of different sizes. In Chapter 5 a summary of the work is given as well as suggestions for further research.

Background

2.1 Introduction

In this chapter previous works on reconfigurable antennas and the methods used to reconfigure these antennas are explored. A survey of journal papers was done to gain some insight into how reconfigurable antennas are being used and to learn the current state of the art. Several reconfiguration techniques have been proposed for the design of these antennas [4]. The most common reconfiguration techniques used are switches. The types of switches that are most commonly used are RF MEMS, PIN diodes and varactors. There are also other methods used for switching such as optical switches [5] and in [6] beam steering was achieved by making use of fluidic actuator. The next section will introduce some of the commonly used methods as a switching element and give examples of how this has been used with reconfigurable antennas as seen in various papers.

2.2 Previous Work

2.2.1 RF MEMS

A MEMS is a microelectromechanical device that uses mechanical movement to achieve a short or an open connection. The operation of a MEMS is similar to a field effect transistor (FET). The terminals are labeled the same as the FET, which are source, gain and drain. Once a DC actuation voltage is applied an electrostatic force pulls the beam into contact with the drain. The RF MEMS requires a high DC actuation voltage to induce the electrostatic force. These devices have low losses, very high isolation and low power consumption [4]. Other advantages of RF MEMS are that they are highly linear and have very high quality factor. They can be designed to handle large RF voltage swings. The high voltage requirements and the lower switching speed may be seen as a drawback. A rectangular spiral antenna with RF MEMS that is capable of changing its radiation pattern is presented in [7]. It was shown that by activating the switches the spiral arm length is changed and results in a change in direction of the radiation beam. Making use of this the antenna was found to provide beam steering capability. The authors of [7] say that this technology could be useful for future reconfigurable antennas and can be used in arrays. The reconfigurable annular slot antenna presented in [8] maintains the same radiation characteristics for both of the operating frequencies. The antenna operates at 2.4 GHz and at 5.2 GHz. The reconfiguration is achieved through the use of single and double arm DC contact MEMS actuators. In the next section work done with PIN diodes as switches for reconfigurable antennas will be presented.

2.2.2 PIN Diodes

A PIN diode is a packaged semiconductor device that has a p-type, I- and n-type region. A high resistivity intrinsic I region is between the p-type and n-type region. Forward biasing the PIN diode results in injecting the -I region with holes and electrons. This will result in an averaged stored charge that persists for a carrier lifetime. Reverse biasing the PIN diode causes a lack of charge in the -I region and the diode appears as a capacitor in shunt with a resistor. PIN diodes need a constant DC current in order to be activated so this should be considered for the biasing of these diodes. The PIN diode can be considered as a current controlled resistor at microwave frequencies. PIN diodes offer the advantage of a faster switching mechanism. Many reconfigurable antennas that use PIN diodes as switches have been proposed. For example, PIN diodes were used as switches to connect four patch sections to a main patch section of a planar antenna in [9]. A field programmable gate array (FPGA) was used to control the activation of the switches. This work showed that using an FPGA to control a reconfigurable antenna is feasible. In [10], a single-feed square-ring patch antenna with switchable radiation pattern is presented. The design uses four shorting walls with two directly connected to the radiating patch. PIN diodes are used to switch the connection state of the other two shorting walls. This antenna allows for its radiation pattern to be switched between conical and broadside radiation. Controlling the states of the diodes the antenna can operate at two different modes. When the PIN diodes are forward biased, they are in the ON state and the antenna operates at the monopolar plate-patch mode which radiates conical patterns. Otherwise the PIN diodes are OFF and the antenna operates at TM11 mode and radiates broadside patterns. In several papers it was shown that PIN diodes could be used for polarization diversity. The polarization diversity is said to be useful in wireless communications applications. In [11], a reconfigurable microstrip antenna with polarization diversity is presented. When the length of the open stub and the ring slot are reconfigured the antenna can switch between circular polarization (CP) and y-directed linear polarization (LP) modes and CP and x-directed LP modes. By reconfiguring the open-stub length and ring slot with two diodes, a LP reconfigurable antenna can be achieved. When a perturbation stub is introduced into the radiating patch of the microstrip the LP antenna can be converted to a switchable CP antenna. It is found that a cross polarization level of less than 20 dB and an axial ratio of less than 3 dB are obtained when the antenna is operated at each LP and CP modes. In [12], a slot-ring antenna with switchable polarization is presented. It is shown that the polarization can be switched between linear and circular polarization by using two PIN diodes. By using four PIN diodes the polarization can be switched between right hand circular polarization (RHCP) and left hand circular polarization (LHCP). Good agreement between the simulation and measurements were found. The polarization diversity could be useful for wireless communication systems. In [4], they simulated and measured a novel reconfigurable slot-ring antenna. They showed that the antenna can be used in an array and that the antenna operates at two frequency bands. By using PIN diode switches the antenna can be operated at 1.76 GHz and 5.71 GHz. In [13], an L-band slot ring antenna that can be reconfigured into a 2 x 2 C-band slot ring antenna that made use of PIN diodes is presented.

2.2.3 Varactor

Varactor diodes are P-N junction diodes that have changing capacitances as the applied bias varies. When a varactor is incorporated into an antenna structure the tuning of the frequency of operation of the antenna can be achieved by tuning the capacitance of the varactor. To tune the capacitance of the varactor a variable voltage source is needed. The biasing lines need to include a RF choke to prevent passage of RF signal to ground. Also, a DC blocker should be included to prevent leakage of DC signal into the antenna structure. In [14], a pattern and frequency reconfigurable array uses varactors to control the phase. In [15], a tunable band notched antenna that makes use of a varactor diode for a frequency tunable patch antenna is discussed. The antenna consists of a bevelled square planar monopole antenna with an embedded rectangular slot ring. The varactor is placed in the resonant slot of the antenna. It is found that the notch can be tuned by making use of a control signal to adjust the DC bias voltage of the varactor. The antenna is found to maintain good radiation performance. An example of using a variable capacitance to vary the input impedance of an antenna is shown in [16]. Here, a frequency tunable microstrip antenna is presented. It is found that adding a U-slot on the patch a flat input resistance and a linear input reactance can be obtained. Varying the matching frequency can be done by adjusting the input reactance. A fabricated prototype is found to attain a tunable frequency from 2.6 to 3.35 GHz. It is shown that using a variable chip capacitor the input impedance of the patch antenna can be controlled.

2.3 Technical Challenges

The incorporation of the switching elements can pose a challenge due to the biasing needed to control the switches. These switch control lines can cause parasitic and mutual coupling effects. In [15], the DC bias voltage was isolated from the RF by using a low pass microstrip filter. Another technical challenge involved is with the feed network used for microstrip arrays. The elements in an array can be fed by using a single line know as a series feed or in multiple lines in a feed network arrangement known as a corporate feed. Figure 2.1 shows examples of the series feed and the corpoarte feed. The corporate feed is ideal for scanning phased arrays, multibeam array or shaped beam arrays [17]. It is know that the radiation from a feed line is a problem that limits the cross-polarization and side lobe level in array [17]. This problem can be addressed by isolating the feed lines form the radiating elements of the array. The spacing between radiating elements in an array need to be considered to avoid direct coupling between the elements as was mentioned in [14].

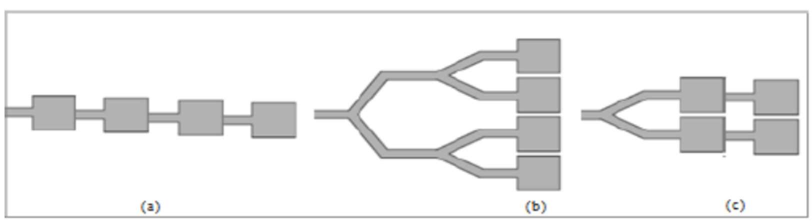

Figure 2.1: (a) series fed array. (b) Multiple feed lines know as corpoate feed. (c). Combination of both feeding techniques. [1]

2.4 Methods of Analysis

In the works surveyed it is found that there are a variety of methods used to make an antenna reconfigurable. Consideration needs to be given to the placement and location of biasing lines. In [13], the dc biasing lines were placed at a location where there is a minimum in the electric field as a way to minimize the interface with the RF performance. Since we are modeling a 2 x 2 array as our unit cell consideration needs to be given to the feed network as well. In order have minimal interference between the radiating elements and the control lines we propose a separate multilayer approach where the radiating elements of the array are separated from the feed and control lines with a ground plane in-between.

2.5 Summary

In this section a brief survey of literature was done and some background was presented into the work being done with reconfigurable antennas. The technical challenges associated with reconfigurable antennas and antenna arrays has been discussed. A lot of the papers surveyed had the biasing control lines and the feed lines on the same plane as the radiating elements. We have chosen to isolate the radiating elements in the array from the feed and control lines to avoid any unwanted coupling.

Methodology

3.1 Proposed study

In this work we are going to present the results of a reconfigurable antenna array model. This will be done through modeling and simulation. The reconfigurable antenna will be modeled for different switching configurations and different array sizes. Various antenna parameters will be reported in the analysis of the array performance. The antenna radiation patterns for each switch configuration are measured and the gain and angle data is used for further analysis. Pattern multiplication will be used to generate radiation patterns of larger arrays. The pattern multiplication model will be compared to the actual data collected from the modeling and simulation done in commercial software. The pattern multiplication model will be done using an isolated unit cell and an embedded unit cell. The pattern multiplication model will be compared to the actual data from simulation in order to see if the effects of mutual couple degrade or distort the radiation pattern.

3.2 Approach

The approach used to model that antenna is presented in this section. In this work we would like to simulate a two-by-two single transceiver array to determine the array patterns under various switching conditions. The synthetic radiation pattern generated from the simulation can be used with pattern multiplication to model larger array sizes. The proposed antenna is a single square spiral microstrip antenna that is based off the work presented by [2]. The single square spiral microstrip antenna is used as a single element of a 2 x 2 array. The 2 x 2 array will be used as a unit cell for larger arrays. Several array sizes will be explored. The antenna is modeled using Cadence's AWR Design Environment. Several larger array sizes are simulated and the data is exported. The data from the unit cell is used to model larger arrays using pattern multiplication. Four elements in a two by two array will have a single transceiver which is corporately fed. The corporate feed technique is used to provide power splits of 2^n [17]. The corporate feed is accomplished by using quarter wavelength impedance transformers at the desired frequency of operation. With the corporate feed method the amplitude and phase of each unit cell can be controlled. AWR Microwave Office is used to model the 2 x 2 array and simulate the performance of the switching conditions. Pattern multiplication is used to model the multifunctional subarray patterns. The pattern multiplication model is an approximation and there is a loss of accuracy due to the asummption of uniform current distribution across the elements.

3.2.1 Single Square Spiral Microstrip Antenna

The single square spiral mircrostip antenna was reported by [2] to reconfigure its radiation pattern and frequency of operation. Figure 3.1 displays the layout of this antenna. The antenna was reported to operate in S band and reconfigure to operate in C band. The antenna makes use of two PIN diodes to change the frequency of operation. Changing the frequency of operation allows the antenna to be scaled for greater spectral coverage. This greater spectral coverage is attractive for several applications. The purpose of of two PIN diodes is to enable and disable different segments of the antenna. These different segments are used to switch the frequency of operation and radiation pattern. The antenna was found to operate at 3.7 GHz and could be reconfigured to operate at 6 GHz. The antenna could also operate at 3.7 GHz but with a changed radiation pattern. Figure 3.2 displays the radiation patterns for each switch state.

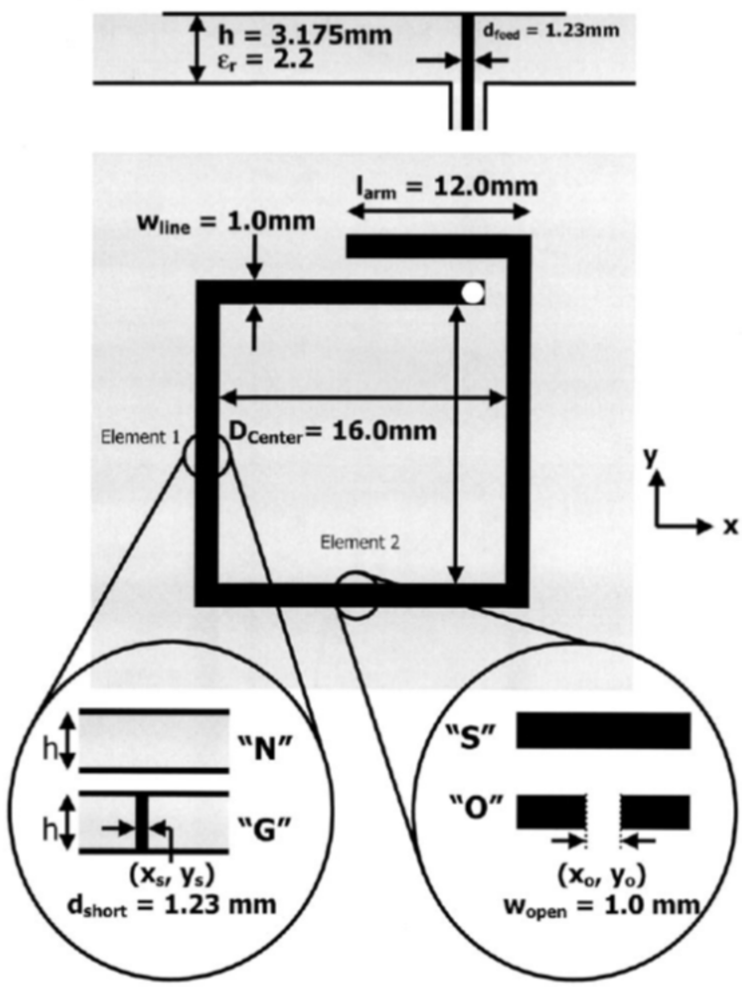

Fig. 1. Antenna geometry showing switches necessary for reconfiguration.

Figure 3.1: Antenna geometry showing the PIN diode placement [2].

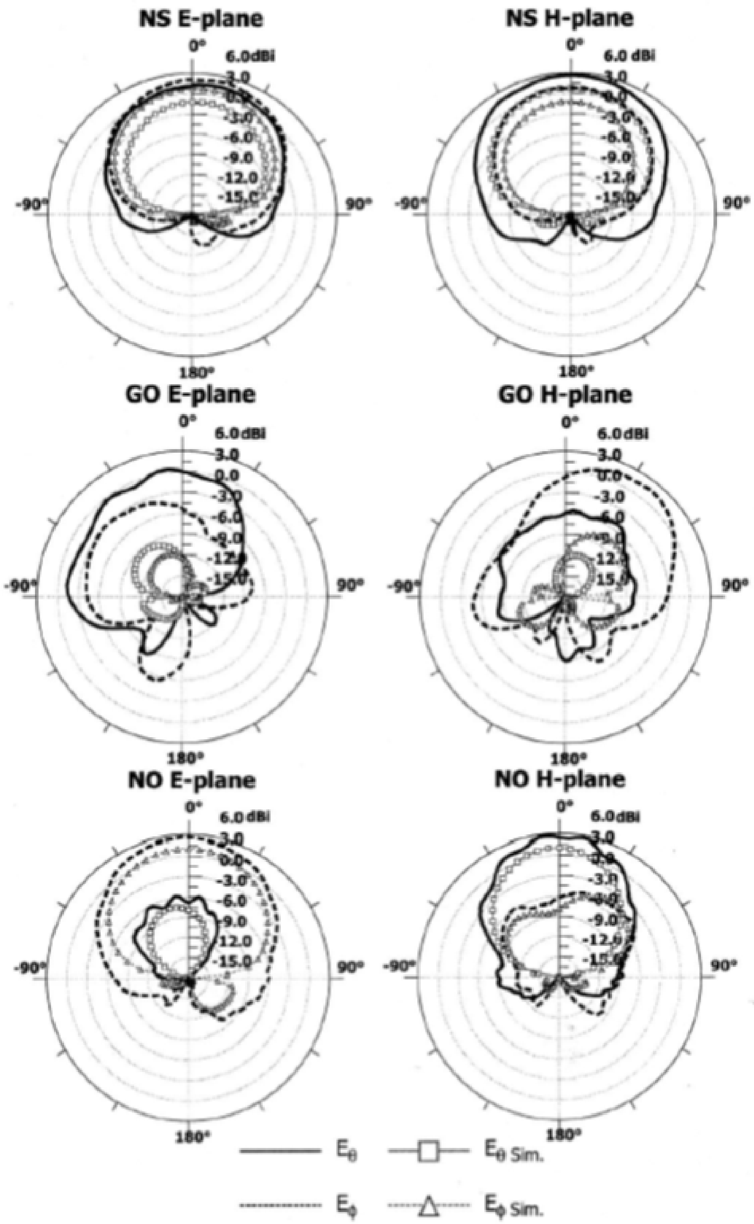

Fig. 4. Measured and simulated gain [dBi] in the E-plane and H-planes for the three configurations.

Figure 3.2: Measured and simulated gain in the E- and H-planes [2].

3.2.2 Array Modeling and Simulation

Cadence's AWR Design Environment 15 is used to model the antenna. The antenna was modeled as an EM structure using the AXIEM EM simulator. The AXIEM EM simulator is a planar 3D Method of Moments asynchronous simulator. The antenna element is modeled using a multilayer stack-up. The stack up is used to define the layers of the stack-up, the material parameters and substrate parameters. The x and y grid size used for meshing is set to 0.1 mm. The model is done using five layers in the stack up. The first layer is the antenna trace, modeled as copper. The second layer is the substrate modeled as RT/Duroid 5880 which has a permittivity of 2.2 and loss tangent 0.0009. The substrate on this layer has a thickness of 3.175 mm. Third layer is a shared ground plane (42 mm $\times$ 46 mm). The shared ground plane separates the radiating elements on top of the first substrate and the feed network located on the bottom of the second substrate. The separation helps with electromagnetic interference between the two layers. The fourth layer is RT/Duroid 5880 with the same parameters and thickness as the second layer of the stack-up. The fifth layer is the feed network. Figure 3.3 presents the unit cell. The unit cell consists of four of the single square spiral microstrip antennas to create a 2 x 2 array. The spacing between elements in the unit cell is 21.0 mm in the x-direction and 23.0 mm in the y-direction.

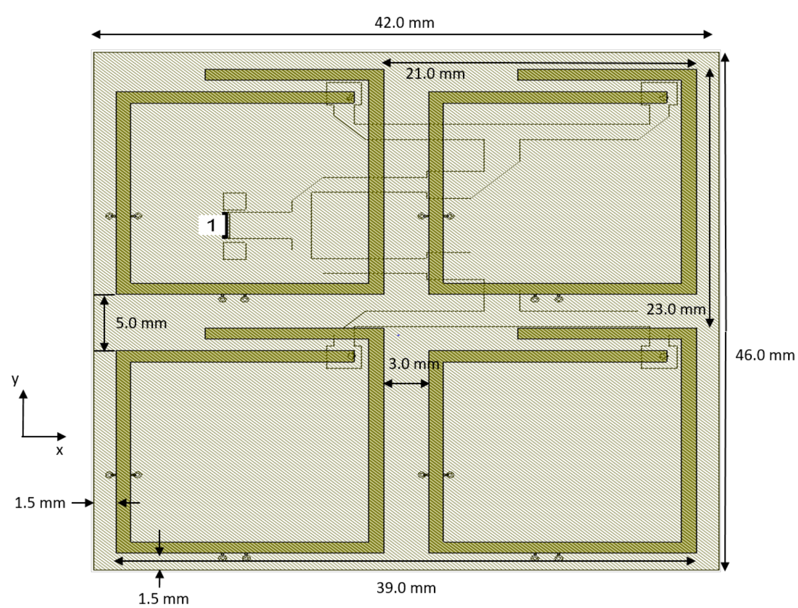

Figure 3.3: Unit cell with dimemsions.

One port is used to feed the four individual single square spiral elements of the unit cell. Each of the unit cells will have its own individual feed. By doing this we are creating a

MIMO array. Each of the four single square spirals of the unit cell are fed with a technique known as a corporate feed. This feed network is used as a way to feed each of the antenna elements individually. The feeding of the individual antenna elements is accomplished by using vias that connect the feed points for each antenna element through the substrate layers and to the feed network. Each of the feeds are excited using a different port in AWR. Figure 3.4 presents the layout of the feed network and the dimensions of the design.

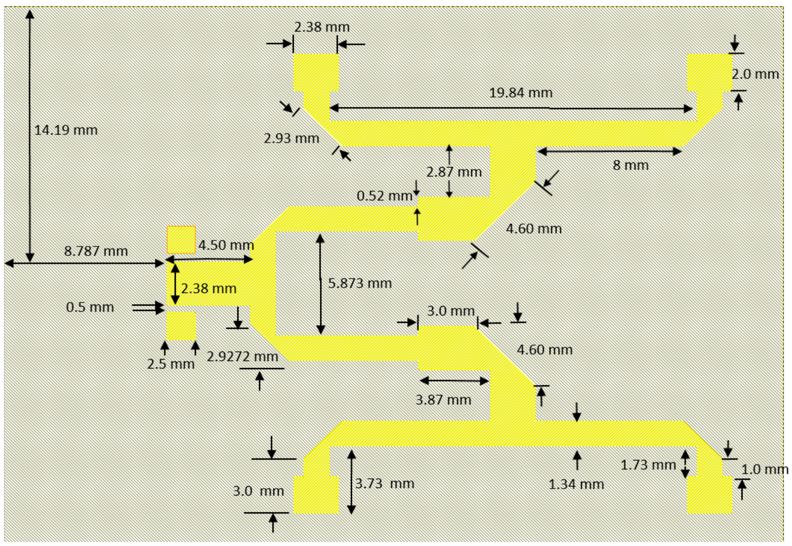

Figure 3.4: Feed network with dimensions.

3.2.3 PIN Diode

The PIN diodes are modeled in the ideal case for each state. The shunt diode is modeled as a short to ground when the diode is on. When this diode is on the short to ground allows the current to be redirected to the ground. The series diode is in line with the trace and allows continuous flow of the current. When this diode is off it is represented as an open in the trace. This open is represented as 1 mm gap in the trace creating two separate segments in the spiral. The open is placed 50 mm from feed point of the spiral antenna. The shunt diode is placed 25 mm from the feed point of the spiral. The PIN diodes will be biased using vias that connect diodes through the substrate and the ground plane. Figure 3.5 displays a side view of the unit cell that was modeled in AWR. Here, the two substrate layers can be seen, along with the vias that connect the feed point and the PIN diodes.

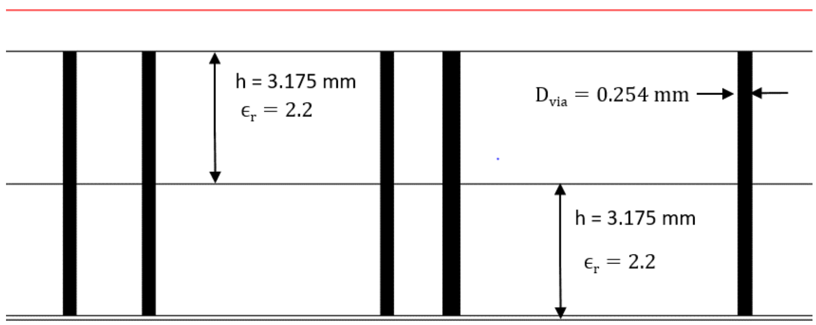

Figure 3.5: Substrate Side View With Dimensions.

3.2.4 Antenna Switch Configurations

The antenna can operate in four different switch configurations. Based off of the naming convention that was used by [2] these switch states are NS, NO, GO and GS. The NS configuration is when the shunt diode is off and the series diode is on. When the antenna is in the NS configuration it has strongest resonance at the frequencies of 3.15 GHz and 8.28 GHz. The NO configuration is when the shunt diode is off and the series diode is on. When the antenna is in this configuration it has strongest resonant at the frequencies at 5.78 GHz and 8.94 GHz. The antenna in the GO configuration is when the shunt diode is on and the series diode is off. When the antenna is in this configuration it has strongest resonance at the frequencies of 5.14 GHz and 9.67 GHz. The antenna in the GS configuration is when the shunt diode is on and the series diode is on. When the antenna is in this configuration it has strongest resonant frequencies at 6.28 GHz and 9.71 GHz. In Figure 4.1 the resonant frequencies of the four switch states can be seen.

3.3 Analysis Methods

3.3.1 Pattern Multiplication

The pattern multiplication model is an approximation of the array pattern. The pattern multiplication model makes the assumption that the current distribution is the same across all of the antenna elements. Using this approximation the array pattern factors as

$$F(\theta, \phi) = f_e(\theta, \phi) AF(\theta, \phi), \tag{3.1}$$

where f_e is the element pattern and AF is the array factor. The radiated pattern is observed in the far field and is the magnitude of the total electric field. $f(\theta, \phi) = |E(\theta, \phi)|$ with angular dependency. The array factor is the array pattern when the array elements are isotropic radiators. An isotropic radiator is a hypothetical lossless antenna having equal radiation in all directions [17]. The array factor of a uniform linear array is

$$AF(\theta, \phi) = |\sum_{n=0}^{N-1} I_0 e^{jk\hat{k}(\theta,\phi)d_n}|^2 \tag{3.2}$$

when the array is a ULA composed of isotropic radiators. The uniform linear array (ULA) is an array whose elements are uniformly spaced along a line. The pattern multiplication model ignores the mutual coupling effects of arrays. Using this model gives us an efficient way to study the antenna performance in digital beamforming applications. Using the synthetic patterns generated from the unit cell we can model larger array sizes using the pattern multiplication technique. The 3D radiation patterns are plotted from the simulated data. Figure 4.5 displays the 3D radation patterns. The data consists of the azimuthal angle θ , the polar angle ϕ and the gain at these angles where, $\phi \in [-180, 180]$ and $\theta \in [0, 180]$ in degress. Both of the angles are stepped in 2 degree increments. The 3D plots are generated by sweeping ϕ at every angle θ. Using AWR we simulate the four switch states of the unit cell and these radiation patterns as the element pattern. In AWR the unit cell is modeled and simulated in the x-y plane. In MATLAB the array is modeled in the y-z plane with azimuth and elevation coordinates. For reference Figure 3.6 presents a coordinate system with the array in the y-z plane used in MATLAB. The position of each unit cell is given by $\mathbf{d_{np}} = -\hat{\mathbf{y}}nd_y - \hat{\mathbf{z}}pd_z$. The elemental spacing is d_y and d_z and $n = 0, \ldots, N_y - 1$, $p = 0, \ldots, N_z{-}1$.

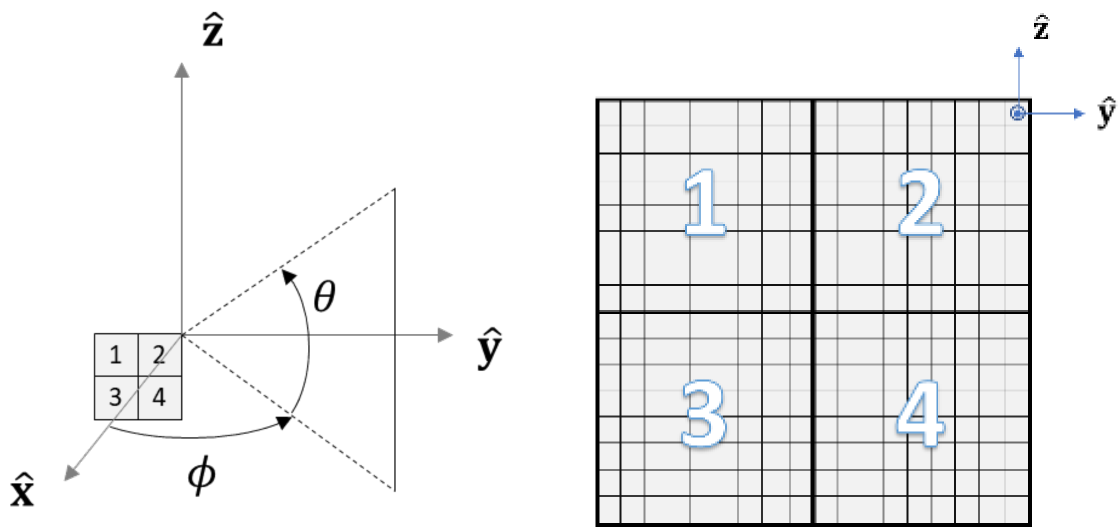

(a) Coordinate system used in MATLAB

(b) Four subarrays in yz-plane

Figure 3.6: Array frame of reference

The signal direction is defined with Cartesian vectors and spherical angle parameters as

$$\hat{\mathbf{u}}(\theta, \phi) = (\hat{\mathbf{x}} \cos(\phi) \cos(\theta) + \hat{\mathbf{y}} \sin(\phi) \cos(\theta) + \hat{\mathbf{z}} \sin(\theta)). \tag{3.3}$$

When the wave arrives off boresight the phase at each element is different but incremental according to the direction of the wave $\mathbf{u}(\theta, \phi)$ and the element position $\mathbf{d}_n$. This is given as

$$\Psi_{np} = k\hat{\mathbf{u}}(\theta, \phi)^T \mathbf{d}_{np}, \tag{3.4}$$

where the wave number $k = 2\pi/\lambda$ and T denotes the vector transpose operator. The array factor is modeled with the azimuth $(\mathbf{a})$ and elevation $(\mathbf{e})$ steering vectors

$$\mathbf{a}(\hat{\mathbf{u}}) = [1, e^{jkd_y \hat{\mathbf{u}}^T \hat{\mathbf{y}}}, \ldots, e^{jkd_y (N_y - 1) \hat{\mathbf{u}}^T \hat{\mathbf{y}}}]^T \tag{3.5}$$

and

$$\mathbf{e}(\hat{\mathbf{u}}) = [1, e^{jkd_z \hat{\mathbf{u}}^T \hat{\mathbf{z}}}, \ldots, e^{jkd_z (N_z - 1) \hat{\mathbf{u}}^T \hat{\mathbf{z}}}]^T. \tag{3.6}$$

For steering the array, a steering vector is defined as

$$\mathbf{v}(\hat{\mathbf{u}}) = \mathbf{e}(\hat{\mathbf{u}}) \otimes \mathbf{a}(\hat{\mathbf{u}}), \tag{3.7}$$

where $\otimes$ denotes the Kronecker vector product. The weighted steering vector in the direction $\hat{\mathbf{u}}_0 = (\theta_0, \phi_0)$ is defined as

$$\mathbf{s}(\hat{\mathbf{u}}_0) = [\mathbf{w}_e \odot \mathbf{e}(\hat{\mathbf{u}}_0)] \otimes [\mathbf{w}_a \odot \mathbf{a}(\hat{\mathbf{u}}_0)], \tag{3.8}$$

where the $\odot$ denotes the Hadamard vector product. The sidelobe levels can be controlled by the weighted azimuth $(\mathbf{w}_a)$ and elevation $(\mathbf{w}_e)$ vectors using a windowing function. The array response in the direction of $\hat{\mathbf{u}}$ is given by

$$F_a(\hat{\mathbf{u}}) = f_e(\hat{\mathbf{u}}) \mathbf{v}(\hat{\mathbf{u}})^H \mathbf{s}, \tag{3.9}$$

where H is the Hermitian transpose.

3.3.2 Embeded Unit Cell

The embedded unit cell used in the pattern multiplication to generate larger arrays will be useful to see the effects of mutual coupling between the elements in the array. The embedded unit cell consists of a 3 x 3 array with only one port being active. Figure 3.7 presents the embedded unit cell. Simulating the array under this condition will allow us to see the effects that mutual coupling is having. The center element of the 3 x 3 array has the active port while the other ports around this one are all off. These elements act as dummy elements in the array. The patterns generated using this as the unit cell will simulate mutual coupling affects.

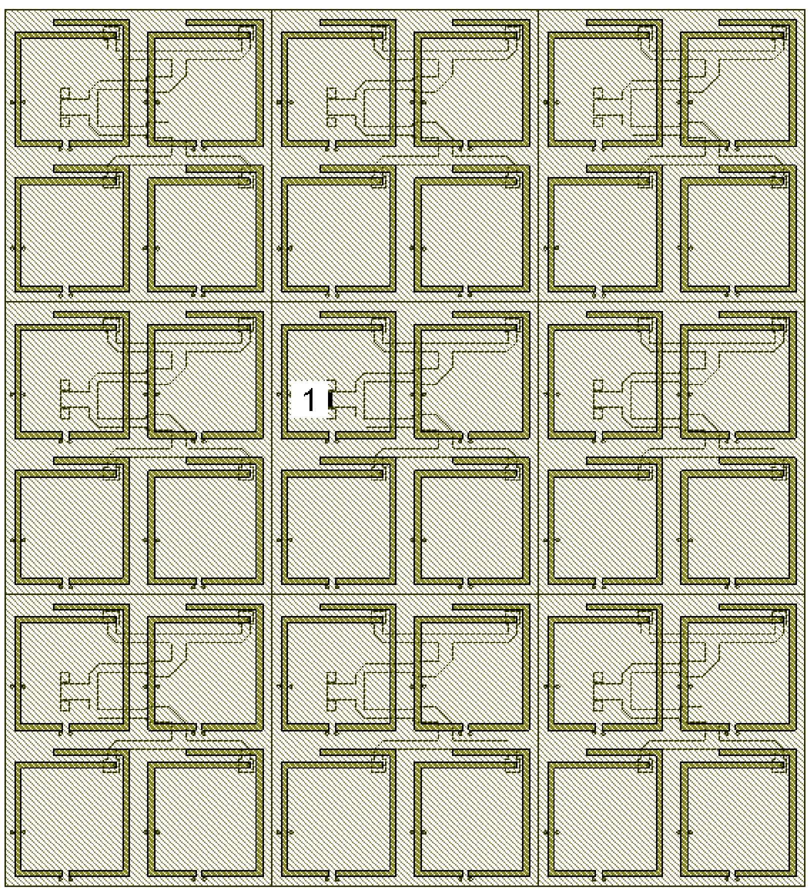

Figure 3.7: Embedded unit cell.

3.3.3 Full Synthesis Model

The full synthesis model comes from the AWR simulations. These simulations account for the active effects of mutual coupling that occurs. The unit cells are simulated for each of the four switch states. Several antenna parameters are reported in Table 4.1 of the results section. This table summarizes the frequncy of operation, 10-dB bandwidth, half-power beam width, S_{11}, voltage standing wave ratio, gain, and directivity. AWR is used to model and simulate larger array sizes as well. In AWR we model up to a 3 x 3 array due to limited computing power. Figure 3.8 displays the 3 x 3 array as modeled in AWR. The 3 x 3 array is a MIMO array that has nine channels.

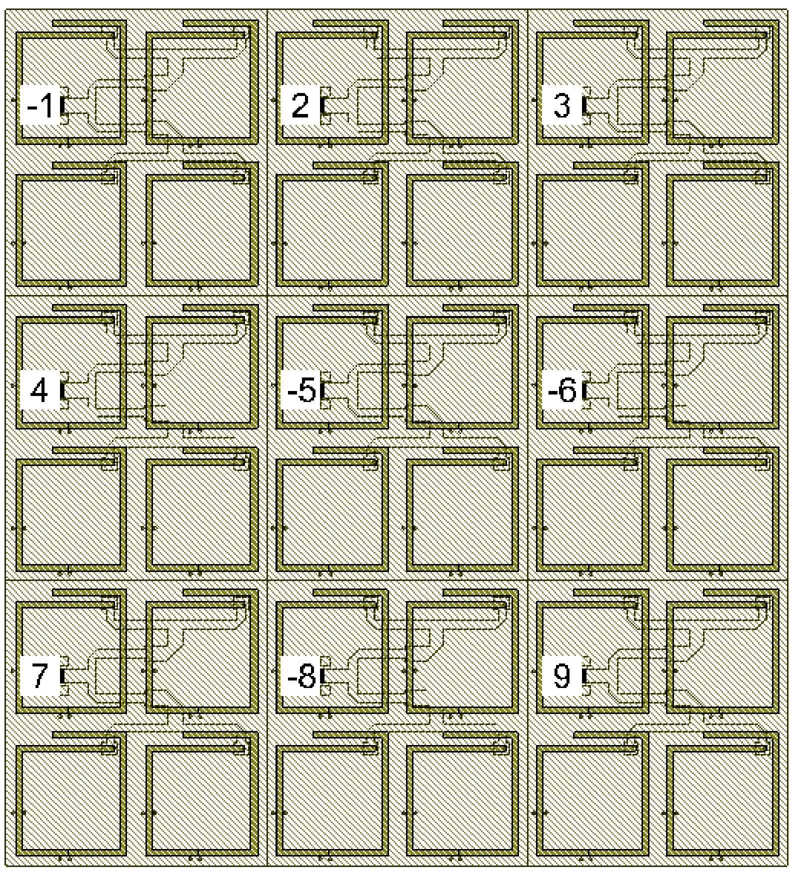

Figure 3.8: Nine channel 3 x 3 array.

3.3.4 Comparison

We want to make a comparison between the pattern multiplication model and the full synthesis model and see how accurate the model is. This can be accomplished by taking the root mean square error between the AWR synthetic array pattern F^{awr} and the isolated and embedded unit cell array patterns F^{iso} and F^{emb}. The RMSE value is

$$RMSE^{x} = [1/Q \sum_{q=1}^{Q} (F_q^{awr} - F_q^{x})]^{1/2}, \tag{3.10}$$

where $F_q^{awr} = F^{awr}(\theta_q, \phi_q)$ is the array patterns from AWR and $F_q^{x} = F^{x}(\theta_q, \phi_q)$ are the embedded or isolated array patterns calculated using Eq. (3.9). Finding the RMSE values between the array patterns can tell us how effective the pattern multiplication model is at representing the array patterns.

3.4 Summary

In this section the proposed study was presented. The approach to modeling and simulation was laid out. The software that was used and the how the model was designed in this software has been explained. The use of the PIN diodes and different switch states were also discussed. Lastly the method of analysis was described. The pattern multiplication model and how it will be used was presented. The use of the isolated and embedded unit cells was explained and how they will be used in comparison with the AWR synthetic array patterns.

Results

4.1 Results

In this chapter we present the overall results of the antenna performance and see how well the pattern multiplication model did. The antenna parameters will be described and the results will be shown. The images of the beam steering will be shown. Then a comparison of the simulated AWR array patterns will be compared with the results of the pattern multiplication using the isolated and embedded unit cells will be given.

4.2 Antenna Performance

Any antenna is characterized by a set of parameters that describes the electrical performance of the antenna [17]. Some commonly reported antenna parameters are the antennas frequency of operation, 10-dB bandwidth, half-power beam width, the reflection coefficient given by the S-parameter S_{11}, voltage standing wave ratio (VSWR), quality factor (Q), gain and directivity. The frequency of operation is the frequency where the antenna has the strongest resonance. The strongest resonance frequency occurs when the S-parameter S_{11} is the lowest value. The antennas reflection coefficient is given in [18] as

$$\Gamma = (Z_{in} – Z_0)/(Z_{in} + Z_0). \tag{4.1}$$

When the voltage source is connected to a transmission line an incident power P_{in} is launched to the input terminals of the antenna. The mismatch of the input impedance of the and Z_{in} and the characteristic impedance of the transmission line Z_0 causes some of the incident power to be reflected back to be reflected back to the source P_{ref} [18]. The portion of the incident power that does not get reflected back is then delivered to the antenna for radiation. The 10-dB bandwidth is given by the span of frequency where the reflection coefficient is in general below -10 dB. The threshold of -10 dB indicates a 30% or less reflection of the incident power at the antenna input terminals [4]. The VSWR is given as [17]

$$VSWR = (1 + |\Gamma|)/(1 - |\Gamma|). \tag{4.2}$$

The VSWR is another meausre of the mismatch of the transmission line. A VSWR of 1 implies a matched load [18]. The antennas quality factor (Q) is the time average of the stored energy around the antenna divided by is radiated power [4]. In general the quality factor is an indication of how the energy inside an oscillating system is dissipating. Lower quality factor means faster energy dissipation which is desirable because this allows for faster radiation of energy. It was reported in [19] that a low quality factor indicates acceptable antenna efficiency. The directivity of the antenna is a directional measure that is defined as a ratio of the radiation intensisty in a given direction from the antenna to the radiation intensity averaged over all directions [17]. The gain of an antenna is closely related to the directivity however, the gain takes into account the reflection and mismatch losses. Gain is a ratio of the radiation intensity in a given direction, to the radiation intensity of an isotropic radiator. The half-power beamwidth is a two sided meausure of the angle that is 3-dB down from the maximum gain. The unit cell was modeled and simulated in AWR for each of the switch states. Table 4.1 presents the antenna parameters. From this table we can see the overall performance of the unit cell for each switch configuration. The antenna in the NS state can be seen to have a frequency of operation at 3.15 GHz with S_{11} of -18.68 dB. The 10-dB bandwidth was measured to be 80.9 MHz. The VSWR was found to be 1.581. The Q for the NS state was found to be -27.65 dB. The antenna in the NO state can be seen to have a frequency of operation at 5.78 GHz with S_{11} of -22.13 dB. The 10-dB bandwidth was measured to be 168.5 MHz. The VSWR was found to be 1.17. The Q for the NO sate was found to be -21.93 dB. The antenna in the GS state can be seen to have a frequency of operation at 6.28 GHz with S_{11} of -21.71 dB. The 10-dB bandwidth was measured to be 104.12 MHz. The VSWR was found to be 1.179. The Q for the NO sate was found to be -11.91 dB.

Table 4.1: Antenna parameters of the unit cell for each of the switch states.

	NS	NO	GS	GO
F (GHz)	3.15	5.78	6.28	5.14
BW (MHz)	80.9	168.5	95.5	171.3
HPBW	88.98	112.29	104.12	56.32
S_{11} (dB)	-18.68	-22.13	-21.71	-17.9
VSWR	1.581	1.17	1.179	1.292
Q (dB)	-27.65	-21.93	-15.78	-11.91
Gain (dB)	6.069	8.853	0.9555	0.5482
Directivty (dB)	7.184	9.387	4.795	3.879

In Figure 4.1 the S_{11} parameter can be seen for the unit cell for all of the switch states. The S_{11} parameter is plotted over a frequency range of 3 GHz – 10 GHz. Each of the four states has more than one acceptable frequency of operation, however we choose to use the frequency that had the strongest resonance.

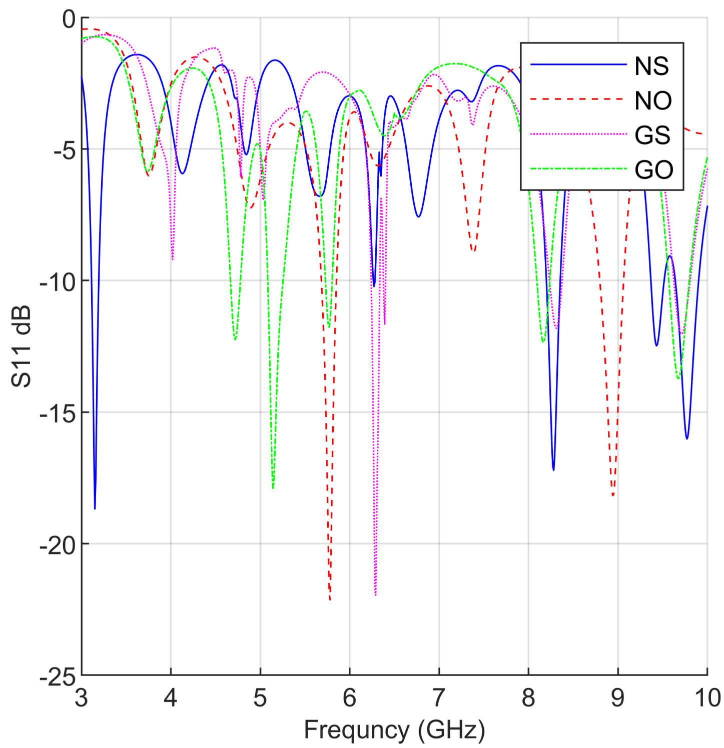

Figure 4.1: S11 in dB of the unit cell for each of the switch states.

In Figure 4.2 the E-Plane and H-Plane gain patterns in dB are displayed for the four states of the antenna. The blue solid line shows the E-plane and the red dashed line is showing the H-plane. Using the AWR coordinate system the E –Plane is designated as the x-z plane with +90 deg as the positive x-axis. The H-plane is designated as the y-z plane with +90 deg as the positive y-axis.

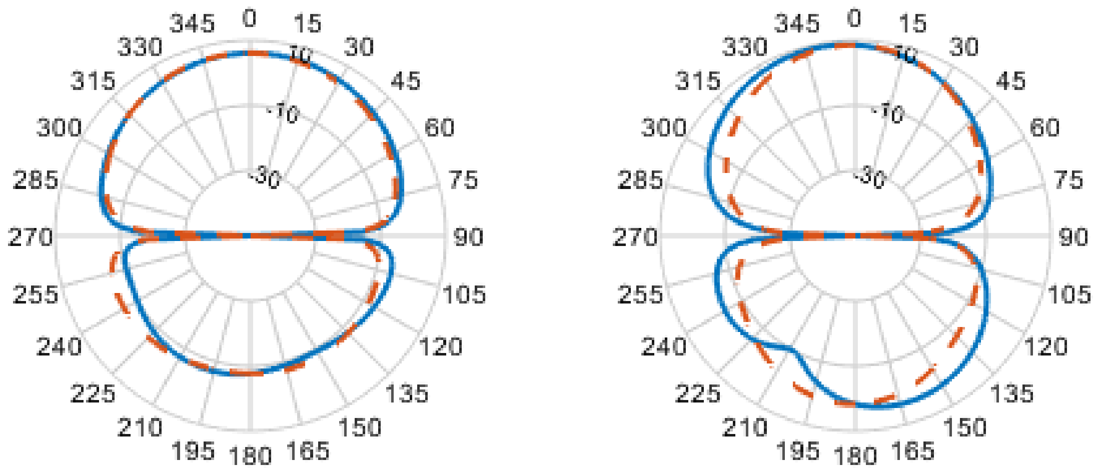

(a) NS at 3.15 GHz.

(b) NO at 5.78 GHz.

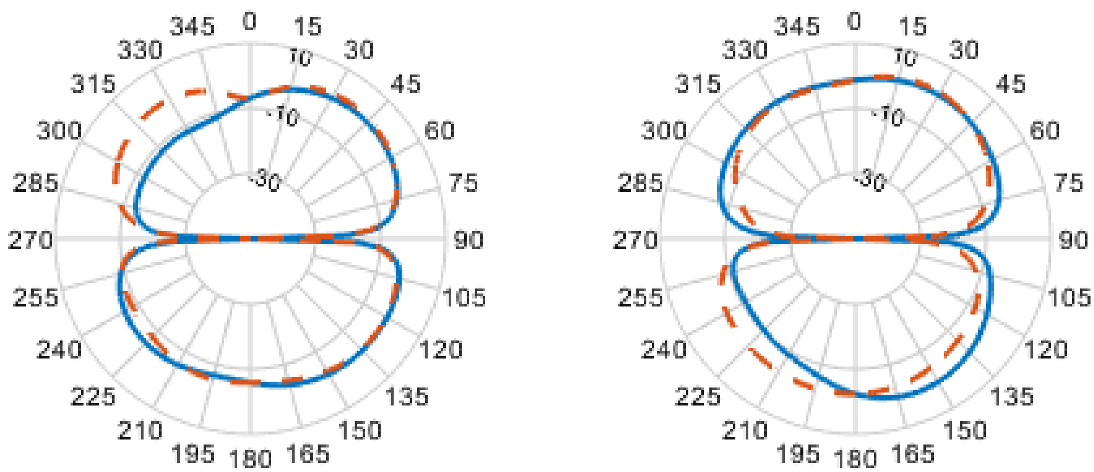

(c) GO at 5.14 GHz.

(d) GS at 6.28 GHz.

Figure 4.2: E-Plane (solid blue line) and H-plane (dashed red line) gain patterns in dB of the unit cell for each of the switch states.

4.3 Received Array Patterns

The received patterns are calculated using Eq. (3.9) in the direction of $\hat{\mathbf{u}} = (\theta, \phi)$. When the weighted steering vector is in the direction $(\theta_0, \phi_0) = (0 \text{ deg}, 0 \text{ deg})$ the array response is in the boresight direction. Figure 4.3 is showing the the 3D radiation patterns for the NS and NO switch states for a 3 x 3 array using the f^{iso} and f^{emb} unit cells. The 3D radiation patterns for the GO and GS switch states for a 3 x 3 array using the f^{iso} and f^{emb} unit cells are shown in Figure 4.4. For both of the figures the array response has not been steered so the signal direction is boresight.

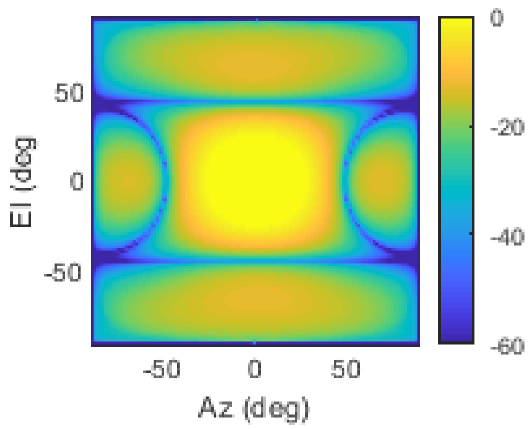

(a) 3 x3 NS isolated unit cell.

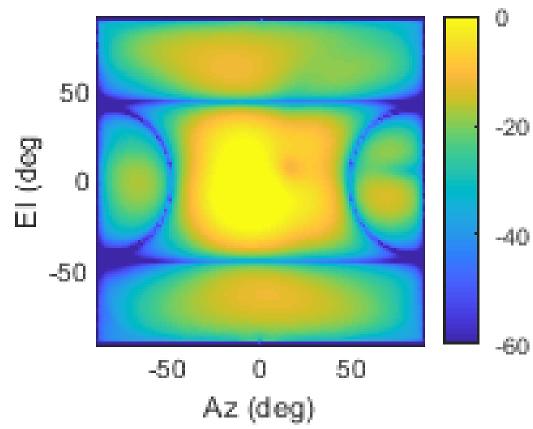

(b) 3 x 3 NS embedded unit cell.

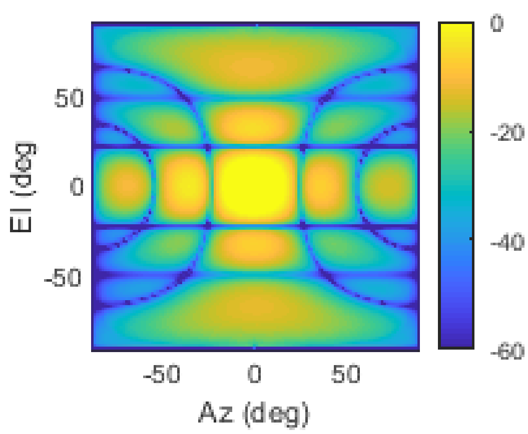

(c) 3 x 3 NO isolated unit cell.

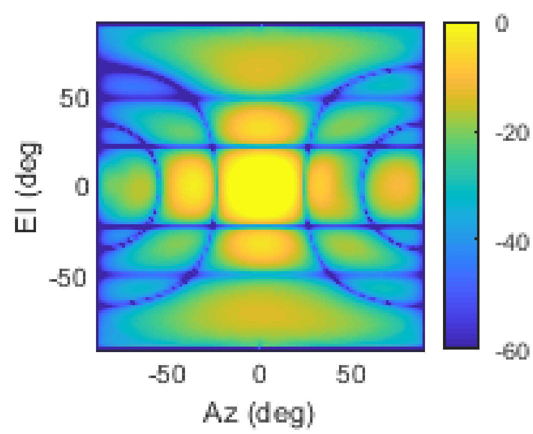

(d) 3 x 3 NO embedded unit cell.

Figure 4.3: 3 x 3 array patterns using f^{iso} and f^{emb} when shunt diode is disabled.

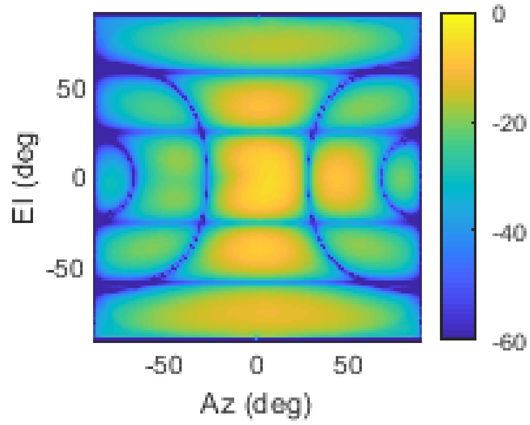

(a) 3 x3 GO isolated unit cell.

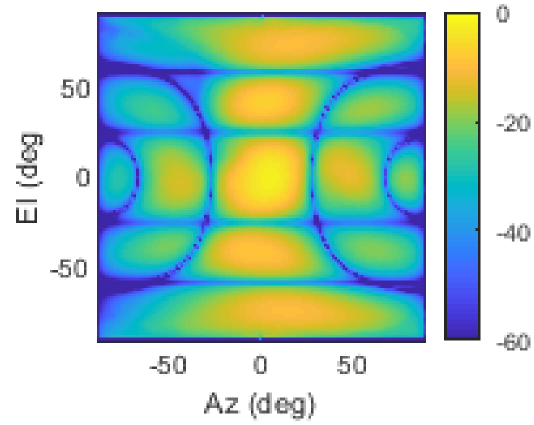

(b) 3 x 3 GO embedded unit cell.

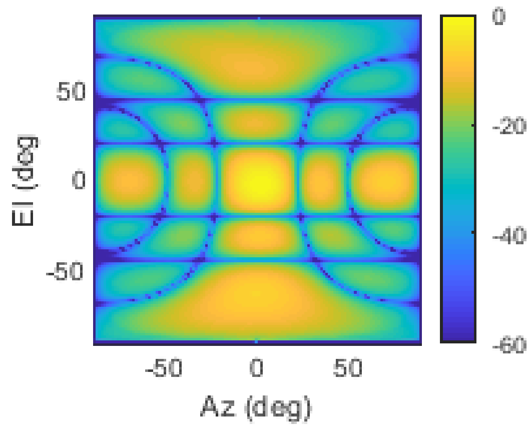

(c) 3 x 3 GS isolated unit cell.

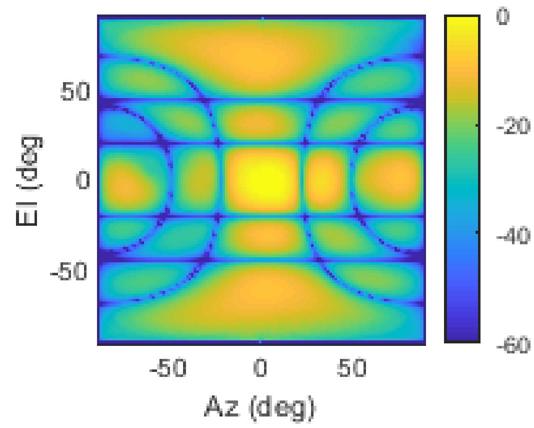

(d) 3 x 3 GS embedded unit cell.

Figure 4.4: 3 x 3 array patterns using f^{iso} and f^{emb} when shunt diode is enabled.

4.4 Beam Steering

The beam steering is achieved by applying a weighted steering vector in the direction $\hat{\mathbf{u}}_{\mathbf{0}}(\theta_0, \phi_0)$. The steering vector is calculated using Eq. (3.7) and the weighted steering vector is calculated using Eq. (3.8). Figure 4.5 shows the normalized 3D gain patterns in dB for an 8 x 8 array. The pixels in Figure 4.5 correspond to a direction $\hat{\mathbf{u}}(\theta, \phi)$ and using Eq. (3.9) the pixel value is calculated. In this case the weights of Eq. (3.8) are steered to boresight ($\theta_0 = 0$ deg, $\phi_0 = 0$ deg). In Figure 4.6, the beam has been steered to an angle ($\theta_0 = 30$ deg, $\phi_0 = 30$ deg).

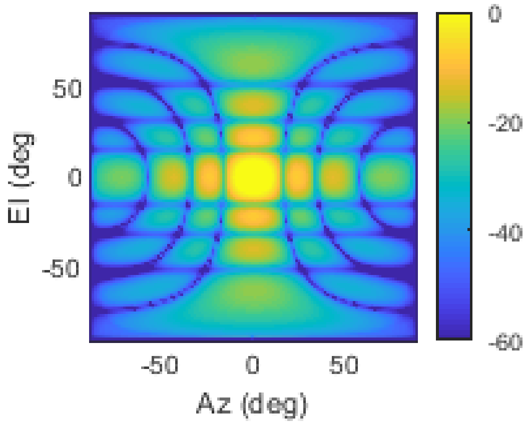

(a) NS

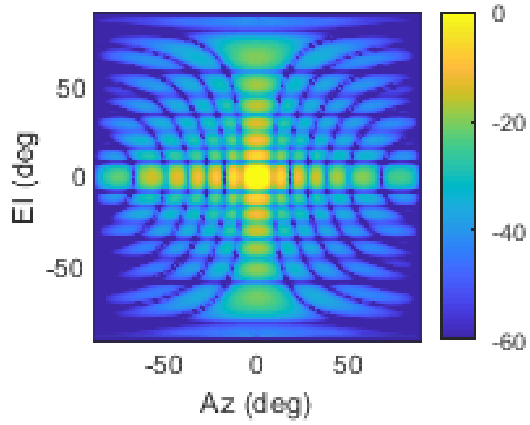

(b) NO

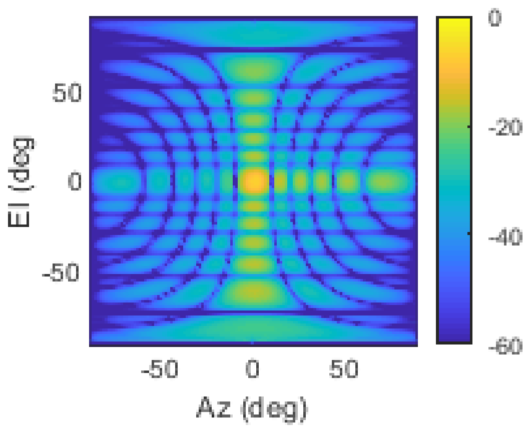

(c) GO

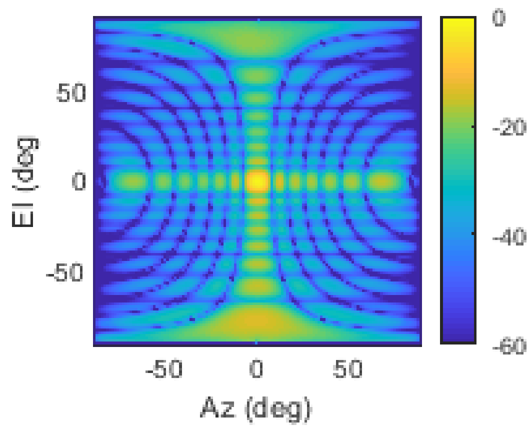

(d) GS

Figure 4.5: Normalized 3D gain pattern in dB for the 8x8 array. The signal is arriving from aspect ($\theta = 0$ deg, $\phi = 0$ deg).

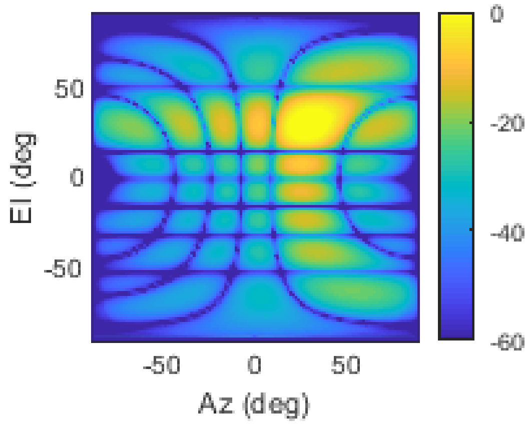

(a) NS

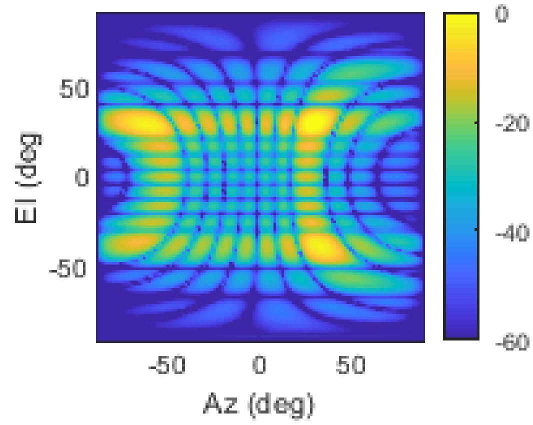

(b) NO

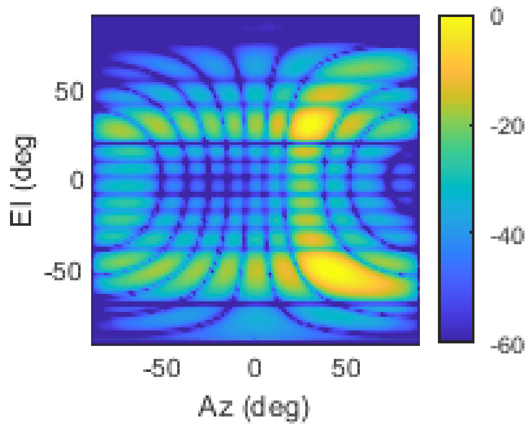

(c) GO

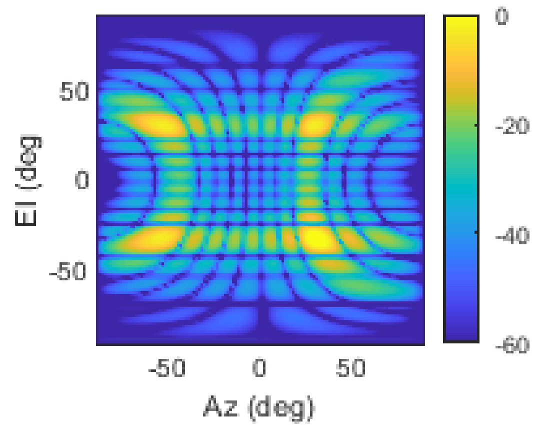

(d) GS

Figure 4.6: Normalized 3D gain pattern in dB for the 8x8 array. The signal is arriving from aspect ($\theta = 30$ deg, $\phi = 30$ deg.)

4.5 Root Mean Square Error

Since the pattern multiplication model ignores the effects of mutual coupling we were interested to see how well the model represents the array patterns. Two find out how much of an effect mutual coupling has on the array patterns we use two different unit cells to build the arrays in the pattern multiplication model. The first unit cell is what we call the isolated unit cell. The isolated unit cell consists of a 2 x 2 array of the single square spiral microstrip which is designated as f^{iso}. The embedded unit cell consists of a 3 x 3 array of unit cells but only the center cell is active. We designate the embedded unit cell pattern as f^{emb}. Simulating the unit cell in this way will capture the effects of mutual coupling on the array pattern. Using the isolated and emebedded unit cells we calculated the array patterns of larger array sizes. Using AWR we simulated the 3D array patterns for several $N \times M$ arrays. Due to the limited computing power the largest array size that could be simulated was a 3 x 3 array. We then compare the AWR array patterns F^{awr} to the F^{iso} and F^{emb} array patterns generated by the pattern multiplication. The patterns are compared using a root mean square error.

In Table 4.2, the results of RMSE for different array sizes for each switch state are presented. In this case, the pattern multiplication was done using the embedded unit cell. Table 4.3 presents the results of the RMSE when the pattern multiplication is done using the isolated unit cell. Table 4.4 highlights the square array cases. Here we can see 2 x 2 and 3 x 3 array with the isolated and embed unit cells. The average RMSE for each switch state are included in the tables as well.

Table 4.2: Root mean square error with embeded unit cell.

N	M	GO	GS	NO	NS
1	1	3.1696e-17	1.6896e-17	1.8782e-17	5.0557e-17
1	2	0.2271	0.1430	0.0762	0.1608
1	3	0.2194	0.1236	0.0861	0.1527
1	4	0.1996	0.1112	0.0844	0.1440
2	1	0.2085	0.1594	0.0980	0.1635
2	2	0.1295	0.0636	0.0236	0.1128
2	3	0.1588	0.0590	0.0356	0.0955
2	4	0.1300	0.0628	0.0447	0.0962
3	1	0.2192	0.1383	0.1018	0.1633
3	2	0.1366	0.0643	0.0387	0.1036
3	3	0.0821	0.0279	0.0084	0.0672
4	1	0.2121	0.1574	0.0975	0.1579
Average	RMSE	0.1602	0.0925	0.0579	0.1181

Table 4.3: Root mean square error with isolated unit cell.

N	M	GO	GS	NO	NS
1	1	6.3850e-17	2.7527e-17	3.1655e-17	6.3246e-17
1	2	0.2405	0.1577	0.0886	0.0992
1	3	0.2331	0.1510	0.0962	0.1329
1	4	0.2095	0.1401	0.0931	0.1365
2	1	0.1998	0.1622	0.0875	0.0959
2	2	0.1165	0.0532	0.0230	0.0259
2	3	0.1648	0.0719	0.0384	0.0607
2	4	0.1352	0.0731	0.0456	0.0795
3	1	0.2149	0.1619	0.0962	0.1307
3	2	0.1335	0.0757	0.0372	0.0544
3	3	0.0902	0.0392	0.0120	0.0077
4	1	0.2094	0.1582	0.0933	0.1361
Average	RMSE	0.1623	0.1037	0.0593	0.0800

Table 4.4: Root mean square error f^{emb} and f^{iso}.

Unit cell	N	M	GO	GS	NO	NS
f^{emb}	2	2	0.1295	0.0636	0.0236	0.1128
f^{iso}	2	2	0.1165	0.0532	0.0230	0.0259
f^{emb}	3	3	0.0821	0.0279	0.0084	0.0672
f^{iso}	3	3	0.0902	0.0392	0.0120	0.0077

Figure 4.7 displays the graph of the RMSE values for each switch state and (N, M) array size. From these results we can that the NO state has the overall lowest RMSE value. This suggests that the effects of mutual coupling is less influential on the array pattern. When the antenna is in the NO state there is an open circuit that leaves the outer winding of the spiral without current flow. This results in very little coupling between the individual elements of the array. When the series diode is on (NS) the current is able to flow through the complete spiral. This results in stronger mutual coupling between the elements in the array. The NS state generally has stronger mutual coupling than the NO state. Overall it seems that the embedded patterns produce a slightly smaller error. For the GO and GS states the RMSE is generally larger than the NO and NS states. The larger RMSE is a

results of the symmetry of the antenna. When the shunt diode is off the current flows in the spiral winding. When the shunt diode is on some of the current flow is redirected to ground. The redirected current disrupts the overall symmetry of the spiral. The lack of symmetry causes a change in the radiation pattern and contributes to a slightly greater mutual coupling effect. This change in the radiation pattern was reported in [2]. From observing the overall data we also noticed that as the array sizes grew larger the difference between the isolated and embedded RMSE values decreased. Form these observations we concluded that the pattern multiplication model is a sufficient way to model larger array sizes.

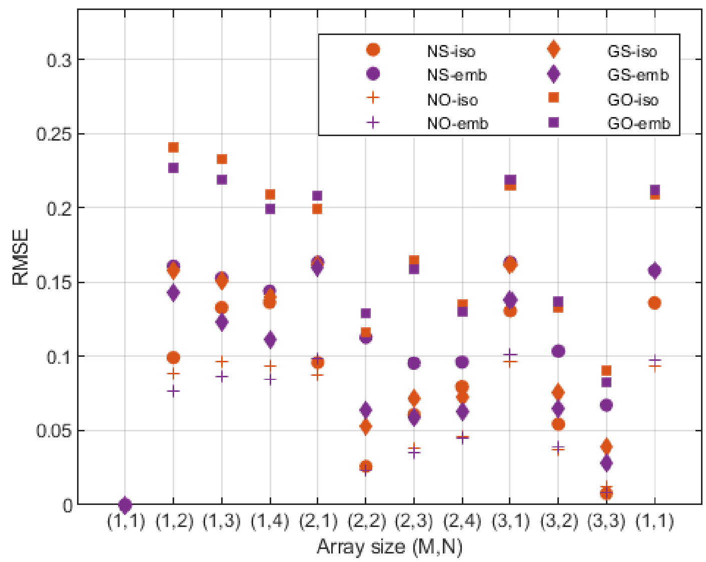

Figure 4.7: S11 of the unit cell for each of the switch states.

4.6 Summary

In this chapter we presented and discussed the results that were obtained during this effort. We highlighted the performance of the antenna for each switch state. Antenna parameters and gain patterns obtained using AWR were shown. We have used the pattern multiplication model to steer the beam of an 8 x 8 array. We collected 3D radiation pattern data from AWR and the pattern multiplication model and compared the synthetic data to the AWR data. The purpose for comparing the radiation patterns produced by AWR and with the isolated and embedded unit cells using pattern multiplication was to see what impact the effects of mutual coupling has on the radiation patterns. The comparisons between the radiation patterns was done by taking a RMSE between the data using different array sizes and the results of this have been presented and discussed.

Conclusions

5.1 Summary

Our goal was to model and simulate a reconfigurable antenna array that could be used as a technology component for cognitive radio system. The reconfigurable antenna is one aspect that makes the cognitive radio possible. We described our approach to building the 2 x 2 unit cell using AWR. Using this unit cell as a single element larger arrays were simulated in AWR up to a 3 x 3 due to limited computing capability. The pattern multiplication model was used to simulate the radiation patterns of larger sized arrays. In order to study the effect that mutual coupling may be having on the pattern multiplication model we chose to use two unit cells to build the arrays. The first unit cell we call the isolated unit cell is the 2 x 2 array of single square spiral microstrip antennas. The second unit cell we call the embedded unit cell which is a 3 x 3 array of the isolated unit cell but only the center excitation port is active and all other ports are off.

We make the comparison between the AWR data and the pattern multiplication model by using a root mean square error (RMSE). We compare 3D array patterns generated from the pattern multiplication model with the AWR radiation patterns. Using the two unit cells several $N \times M$ arrays are simulated. First we compare the NO and NS states. We note that overall the results of the RMSE for the embedded unit cell are smaller. The NO state produces a lower RMSE than the NS state. When the antenna is in the NO switch state the series diode is off. This creates an open in the antenna spiral trace resulting in two separate segments. Due to the open in the circuit there is no current flow in the outer winding of the spiral. This results in very little coupling between the individual elements of the unit cell. When the antenna is in the NS switch state the series diode is on. When the series diode is on the current can flow through the full spiral. This results in stronger coupling between the neighboring elements in the unit cell. Next we make the comparison between the GO and GS switch state. We see that the RMSE values for GO and GS are generally larger than the NO and NS states. When the shunt diode is on a portion of the current is redirected to ground. This redirection of the current flow disturbs the overall symmetry of the unit cell. This lack of symmetry changes the radiation pattern and contributes to an increase in the mutual coupling. We noticed that as the array size increases the difference in RMSE between the isolated and embedded unit cells decreases. Based on the RMSE results we have found that the mutual coupling has a small effect on the radiation patterns and therefore the pattern multiplication model is sufficient to model the array.

5.2 Recommendations for future work

The pattern multiplication model is sufficient to use to create training data for a machine learning controller. Further work is being done with the reconfigurable antenna array that was presented. In a separate work [20], the pattern multiplication model is used to train a neural network to predict the array settings that achieve a desired array pattern. The antenna could be fabricated and measurements could done on the antenna for comparing the measured and simulated results.

Bibliography

[1] K. V. Gohil, M. Prajapati, and F. Paval, “Design of microstrip patch array for gain enhancement using paper substrate,” *Journal of Advances and Scholarly Researches in Allied Education*, vol. 16, no. 3, pp. 248–252, March 2019.

[2] G. H. Huff, J. Feng, and J. T. Bernhard, “A novel radiation pattern and frequency reconfigurable single turn square spiral microstrip antenna,” *IEEE Microwvae and Wireless Components Letters*, vol. 13, no. 2, pp. 57–99, February 2003.

[3] Y. Kok-Lim. Alvin, P. Komisarczuk, and P. D. Teal, “A context-aware and intelligent dynamic channel selection scheme for cognitive radio networks,” in *4th International Conference on Cognitive Radio Orinted Wireless Networks and Communications*, Hannover, Germany, 2009, pp. 1–6.

[4] Y. Tawk, J. Constantine, and C. Christodoulou, *Antenna Desing for Cognitive Radio*. Artech House, 2016.

[5] G. P. Jinr, D. Zhange, and R. L. Li, “Optically controlled reconfigurable antenna for cognitive radio applications,” *IET Electronic Letters*, vol. 47, no. 17, pp. 948–950, August 2009.

[6] S. J. Mazlouman and et. al., “Beam steering antenna using bending fluidic actuators,” *IEEE Transactions on Antenna and Propagtion*, vol. 61, no. 10, pp. 5287–5290, October 2013.

[7] C. Jung, M.-J. Lee, and F. De Flavis, "Reconfigurable scan-beam single-arm spiral antenna integrated with rf-mems switches," *IEEE Transactions on Antennas and Propagation*, vol. 54, no. 2, pp. 455–463, Februrary 2006.

[8] B. Cetiner, G. R. Crusats, L. Jofre, and N. Biyikh, "Rf mems integrated frequency reconfigurable annular slot antenna," *IEEE Transactions on Antennas and Propagation*, vol. 58, no. 3, pp. 626–632, March 2010.

[9] S. Shelley, J. Constantine, C. G. Christodoulou, D. E. Anagnostou, and J. C. Lyke, "Fpga-controlled switch-reconfigurable antenna," *IEEE Antennas and Wireless Propagation Letters*, vol. 9, no. 1, pp. 355–358, May 2010.

[10] S.-H. Chen, J.-S. Row, and K.-L. Wong, "Reconfigurable square-ring patch antenna with pattern diversity," *IEEE Transactions on Antennas and Propagation*, vol. 55, no. 2, pp. 472–475, February 2007.

[11] S.-H. Chen and J.-S. Row, "Single-fed microstrip patch antenna with switchable polarization," *IEEE Transactions on Antennas and Propagation*, vol. 56, no. 4, pp. 922–926, April 2008.

[12] M. K. Fries, M. Grani, and R. Vahldieck, "A reconfigurable slot antenna with switchable polarization," *IEEE Microwave and Wireless Components Letters*, vol. 13, no. 11, pp. 490–492, November 2003.

[13] M. Shirazi, J. Huang, T. Li, and X. Gong, "A switchable-frequency slot-ring antenna element for designing a reconfigurable array," *IEEE T Antennas and Wireless Propagtion Letters*, vol. 17, no. 2, pp. 229–233, Februrary 2018.

[14] N. M. Zainarry, Siti, N. Nquyen-Trong, and C. Fumeaux, "A frequency- and pattern-reconfigurable two-element array antenna," *IEEE Antennas And Wireless Propagtion Letters*, vol. 17, no. 4, pp. 617–620, April 2018.

[15] E. Antonino-Davi, M. Cabedo-Fabres, M. Ferrando-Bataller, and A. Villa-Jimenez, "Active uwb antenna with tunable band-notched behavior," *Electronics Letters*, vol. 43, no. 18, pp. 1–2, August 2007.

[16] S. Yang, S-L, A. Kishk, A, and K.-F. Lee, "Frequency reconfigurable u-slot microstrip patch antenna," *IEEE Antennas And Wireless Propagtion Letters*, vol. 7, pp. 127–129, January 2008.

[17] C. Balanis, *Antenna Theory: Analysis and Design*. New York: John Wiley & Sons, 2005.

[18] D. Pozar, *Microwave Engineering*. New York: John Wiley & Sons, 2012.

[19] B. A. Kramer and et. al., "Fundamental limits and design guidelines for miniaturizing ultra-wideband antennas," *IEEE Antennas and Propagation Magazine*, vol. 51, no. 4, pp. 57–69, August 2009.

[20] C. M. Stamper, G. A. Harris, M. A. Saville, and T. Quach, "Machine learning control of a reconfigurable antenna array for dual-band communications," *Applied Computational Electromagnetics Society*, in review.